Glucosylation of Ras by *Clostridium sordellii* Lethal Toxin: Consequences for Effector Loop Conformations Observed by NMR Spectroscopy†

Matthias Geyer,‡ Christian Wilde,§ Jörg Selzer,§ Klaus Aktories,*,§ and Hans Robert Kalbitzer*,||

Max-Planck-Institut für molekulare Physiologie, Abteilung Physikalische Biochemie, Otto-Hahn-Strasse 11, D-44227 Dortmund, Germany, Institut für Experimentelle und Klinische Pharmakologie und Toxikologie der Albert-Ludwigs-Universität Freiburg, Otto-Krayer-Haus, Albertstrasse 25, D-79104 Freiburg, Germany, and Institut für Biophysik und Physikalische Biochemie der Universität Regensburg, Universitätstrasse 31, D-93053 Regensburg, Germany

Received April 3, 2003; Revised Manuscript Received July 23, 2003

ABSTRACT: The lethal toxin (LT) from *Clostridium sordellii*, which belongs to the family of large clostridial cytotoxins, acts as a monoglucosyltransferase for the Rho subfamily GTPase Rac and also modifies Ras. In the present study we investigated structural changes of H-Ras in its di- and triphosphate form that occur upon glucosylation of the effector domain amino acid threonine-35 by LT. ^{31}P NMR experiments recorded during the enzymatic glucosylation process, using UDP-glucose as a cosubstrate, show that the modification of the threonine side chain influences the chemical shifts of the phosphate groups of the bound nucleotides. In the diphosphate-bound form (Ras·GDP) glucosylation of Thr35 induces only small changes in the chemical environment of the active center. In the triphosphate form with the GTP analogue GppNHp bound (Ras·GppNHp) Ras shows at least two different conformations in the active center that exchange on a medium-range time scale (10 to 0.1 ms). Glucosylation selectively stabilizes one distinct conformation of the effector loop (state 1) with tyrosine-32 probably apart from the nucleotide and threonine-35 not involved in magnesium ion coordination. This conformation is known to have a low affinity to effector proteins such as Raf-1, AF-6, or Byr2 and thus prevents the transduction of the activation signal in the Ras-mediated pathway. NMR correlation spectra of Ras(T35glc)·GDP and denaturation experiments with urea indicate that the glucose is bound in the α-anomeric form to the hydroxyl group of the threonine-35 side chain. Inhibition of the glucosylation reaction by 1,5-gluconolactone suggests a stereospecific reaction mechanism with a glucosyl oxonium ion transition state for the enzymatic activity of LT.

Lethal toxin (LT)[1] from *Clostridium sordellii* is a major virulence factor that is causally involved in diarrhea and enterotoxemia in domestic animals and in gas gangrene in man (*1*). LT has a molecular mass of 270 kDa and belongs to the family of large clostridial cytotoxins (for reviews see refs *2* and *3*). The most prominent members of this toxin family are the *Clostridium difficile* toxins A and B, which are the causative agents of antibiotic-associated diarrhea and pseudomembranous colitis (*4*, *5*). The protein toxins function by transfer of a glucose molecule (LT and *C. difficile* toxins) (*6*, *7*) and an *N*-acetylglucosamine group (*Clostridium novyi* α-toxin) (*8*), respectively, to a threonine residue of their substrate proteins. While *C. difficile* toxins A and B (e.g., from strain VPI 10468) and *C. novyi* α-toxin glucosylate the low molecular mass GTP-binding proteins of the Rho subfamily, Rho, Rac, and Cdc42 (*6*, *8*), lethal toxin modifies not only Rac from the Rho subfamily but also Ras, Ral, and Rap from the Ras subfamily. However, toxin B variants have been described which share the substrate specificity of LT and are capable of modifying Ras subfamily GTPases (*2*). The target site of the monoglucosylation reaction in the small GTPases is a highly conserved threonine residue in the so-called effector loop or switch I region that is sensed for GDP to GTP exchange and involved in the interaction with effector proteins. The threonine residue, which corresponds to Thr35 in the Ras protein and Thr37 in Rho, is involved in magnesium ion coordination by its side-chain hydroxyl group (*9*).

Ras proteins are essential for the regulation of cell differentiation and proliferation. By cycling between a GDP-bound inactive state and a GTP-bound active state, they are involved in the transduction of extracellular signals to the nucleus. The glucose moiety at Thr35 renders Ras inactive, as has been shown by inhibition of the downstream MAP-kinase pathway (*7*, *10*). The functional consequences of glucosylation on the Ras GTPase cycle have been studied

† M.G. thanks Roger S. Goody for support. H.R.K. is grateful to the European Union for supporting this work.

* To whom correspondence should be addressed. H.R.K.: tel, +49-941-943-2594; fax, +49-941-943-2479; e-mail, hans-robert.kalbitzer@biologie.uni-regensburg.de. K.A.: tel, +49-761-203-5301; fax, +49-761-203-5311; e-mail, klaus.aktories@pharmakol.uni-freiburg.de.

‡ Max-Planck-Institut für molekulare Physiologie.

§ Universität Freiburg.

|| Universität Regensburg.

[1] Abbreviations: NMR, nuclear magnetic resonance; Ras, protein product of the H-ras proto-oncogene; LT, *Clostridium sordellii* lethal toxin; RBD, Ras-binding domain; GAP, GTPase-activating protein; GEF, guanosine nucleotide exchange factor; GppNHp, guanosine 5′-*O*-(*β*,*γ*-imidotriphosphate); GTP*γ*S, guanosine 5′-*O*-(3-thiotriphosphate); TOCSY, total correlation spectroscopy; NOESY, nuclear Overhauser effect spectroscopy; DSS, sodium 2,2-dimethyl-2-silapentane-5-sulfonate.

10.1021/bi034529v CCC: $25.00
Published on Web 09/26/2003

recently (*11*). The monoglucosylation of Ras does not significantly alter nucleotide binding properties, whereas the intrinsic GTPase activity was markedly decreased. While the GEF-catalyzed loading with GTP was reduced by glucosylation but not completely inhibited, the GAP-stimulated GTPase activity was completely blocked due to the inability of glucosylated Ras-GTP to bind GAP. The most crucial step in downstream signaling, however, was completely blocked since the affinity of the Ras·GTP complex with the Ras-binding domain (RBD) of the Raf kinase was decreased upon glucosylation by a factor of at least 10^5 (*11*). The X-ray structure of Ras·GDP modified by LT was published recently (*12*). It shows that Thr35 is modified with the glucose bound in its α-anomeric configuration and that the spatial structure of Ras·GDP is only minimally disturbed upon this modification.

We have previously found that the effector loop of Ras bound to the triphosphate analogue GppNHp exists in two distinct conformations (states 1 and 2) that exchange on the millisecond time scale and that are almost equally populated (*13*). Binding to Raf-RBD selectively stabilizes one conformation (state 2), which corresponds to the three-dimensional structures determined for Ras in complex with effector molecules (*14*). In the present paper we correlate the data obtained in the solid state for Ras·GDP with those observed in solution by NMR spectroscopy. In addition, we investigate if the triphosphate-bound Ras·GppNHp can be efficiently monoglucosylated at Thr35 and analyze the influence of this modification on the conformational substates of the effector loop. Since crystallization of Ras could select Ras with one of the two possible configurations, NMR spectroscopy should also be the method of choice to exclude or prove a possible racemisation at the glycosidic bond in solution and thus to estimate the degree of stereospecificity of the LT reaction.

EXPERIMENTAL PROCEDURES

Protein Expression and Purification. Recombinant truncated Ras protein (1−166) was expressed in *Escherichia coli* and purified as described (*9*). Purified GDP, GTP, GTPγS, and GppNHp reagents were purchased from Sigma. GDP, which binds very tightly to Ras, was replaced with the respective nucleoside triphosphate by the following procedures. For nucleotide exchange with GppNHp the substrate was incubated at 3-fold molar excess with Ras in the presence of 200 μM ammonium sulfate, 0.1 μM zinc chloride, and 1 unit of alkaline phosphatase/mg of Ras overnight at 4 °C. To load Ras with GTP or GTPγS, nucleotide-free Ras was produced by overnight incubation at 4 °C in the presence of 200 μM ammonium sulfate, 0.1 μM zinc chloride, and 0.2 unit of alkaline phosphatase/mg of Ras. After size exclusion chromatography, one of the nucleotides was then added to the Ras protein. Excess nucleotide after either procedure was removed by gel filtration in order to obtain accurate NMR spectra for kinetic evaluation. The pooled Ras fractions were concentrated to 20 mg/mL by centrifugal concentrators (Vivaspin 10 kDa cutoff, VivaScience). The buffer used in all of these procedures contained 40 mM Tris-HCl at pH 7.4, 2.5 mM $MgCl_2$, and 1 mM DTE. Lethal toxin (LT) from *C. sordellii* was prepared from strain 6018 as described earlier (*7*) and concentrated to 0.04 μM in 50 mM Tris-HCl at pH 7.6, 5 mM $MgCl_2$, and 500 mM NaCl.

Preparation of the NMR Samples. To monitor the time course of modification and changes in the active center of the protein by ^{31}P NMR spectroscopy, the glucosylation reaction of Ras by LT was performed in the NMR tube. Usually, ^{31}P NMR spectra were recorded in 8 mm NMR tubes (Shigemi) containing 800 μL of the Ras−nucleotide complex with a concentration of 0.4−1.1 mM. To an initial volume of 250−400 μL of highly concentrated Ras protein, 8−16 μL of a solution of 100 mM UDP-glucose, 27 μL of 100 mM $MgCl_2$, 35 μL of 3 M KCl, and 250 μL of 0.04 μM LT was added. A total volume of 800 μL was obtained by adding appropriate amounts of water. To provide a lock signal, the samples contained 10% D_2O. The glucosylation of Ras·GDP was performed twice at 10 and 20 °C with either a 2-fold excess of UDP-glucose relative to Ras or a small excess of Ras relative to UDP-glucose. For Ras·GppNHp the glucosylation reaction was performed three times in the NMR tube at temperatures of 5, 15, and 20 °C and an excess of the UDP-glucose.

Proton NMR experiments on nonmodified Ras·GDP and monoglucosylated Ras(T35glc)·GDP were performed in order to determine the anomeric conformation of the covalently bound hexose. First, the glucosylation reaction of ∼10 mg of Ras·GDP at 20 °C was followed by ^{31}P NMR as described above. Maximum glucose incorporation was achieved after ∼16 h. To remove free UDP-glucose, the protein sample was then placed in a glass dialysis cell and dialyzed three times for 4 h at 4 °C against 2 L of 50 mM Tris-HCl (pH 7.0) and 5 mM $MgCl_2$ but without DTE added. The protein was finally freeze-dried, stored, and redissolved in 250 μL of 99.8% D_2O (Roth, Karlsruhe). For protein denaturation experiments increasing amounts of urea were added. To minimize protonation of the sample, the urea used had been dissolved several times in D_2O and freeze-dried.

Inhibition Studies of the Toxin-Induced Glucosylation with Gluconolactone. For studying the effects of 1,5-gluconolactone on the lethal toxin-catalyzed glucosylation of H-Ras, 10 nM toxin was incubated with ∼3 μM H-Ras, 10 μM UDP-[^{14}C]glucose, and increasing concentrations of gluconolactone or glucose for 15 min at 37 °C. Thereafter, labeled protein was separated by SDS−PAGE, and the amount of incorporated radioactivity was determined by phosphorimaging.

NMR Spectroscopy. ^{31}P NMR experiments were performed on a Bruker AMX-500 NMR spectrometer working at a phosphorus resonance frequency of 202 MHz. The ^{31}P spectra were referenced to 85% phosphoric acid contained in a glass sphere, which was immersed in the sample and calibrated for various temperatures. Unless noted otherwise, phosphorus spectra were recorded at 5 °C with a total spectral width of 60 ppm. For one-dimensional ^{31}P NMR spectra 512−16384 free induction decays were summed after excitation with a 65 deg pulse using a repetition time of 3−5 s. A total of 32 K time domain data points were recorded and transformed to 16 K real data points corresponding to a digital resolution of 0.74 Hz/point.

One- and two-dimensional ^{1}H NMR spectra were performed on a Bruker AMX-500 and a Bruker DMX-800 NMR spectrometer. Two-dimensional NMR spectra were recorded in the phase-sensitive mode, and the water signal was suppressed by selective presaturation during the preparation period and/or mixing time. Typically, spectral widths were

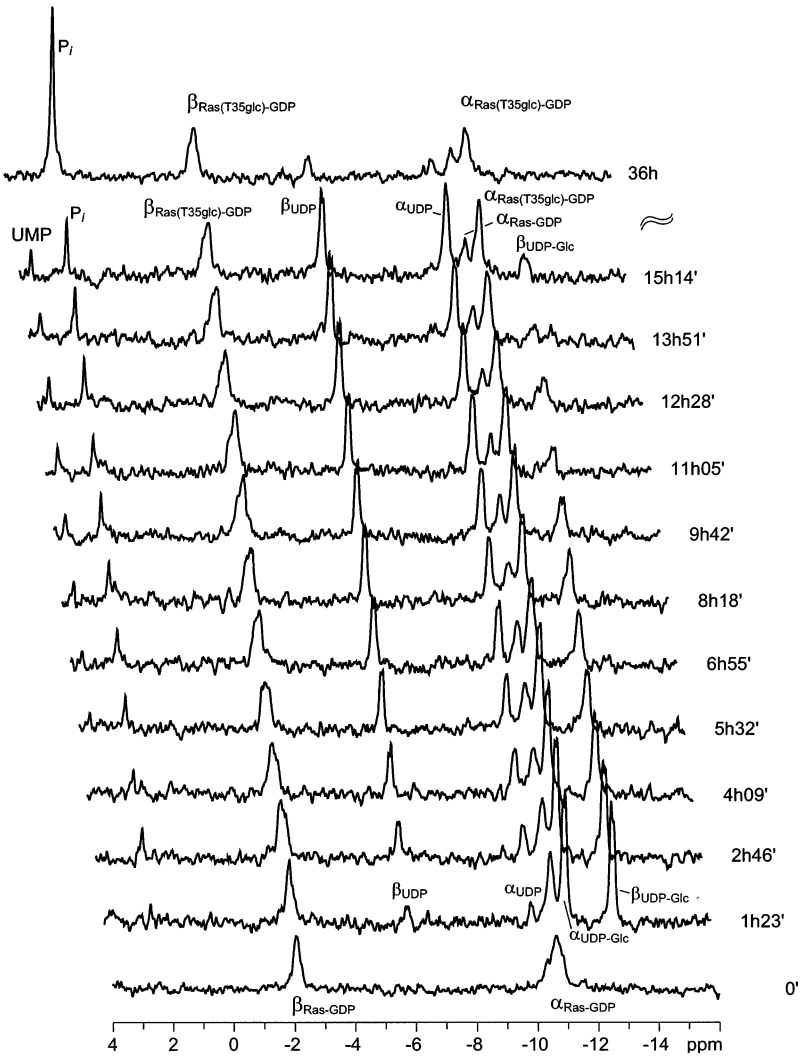

FIGURE 1: Monoglucosylation of Ras·GDP·Mg^{2+} by LT as observed by ^{31}P NMR. Spectra were recorded at 20 °C in 20 mM Tris-HCl buffer, pH 7.4. The total protein concentration was 0.47 mM Ras·GDP·Mg^{2+} and 11.4 nM LT toxin using a buffer of 0.8 mM UDP-glucose, 5 mM $MgCl_2$, and 120 mM KCl in 875 μL of water (H_2O/D_2O, 90%/10%). Each single spectrum was recorded with 1200 scans corresponding to 83 min each. Note the small shift upon glucosylation in the Ras·GDP β-resonance line position (−2.1 ppm) and the increasing signals of UDP (α_{UDP}, −10.1 ppm; β_{UDP}, −6.1 ppm).

15.1 ppm, and the carrier was positioned at the solvent signal. Homonuclear TOCSY and NOESY experiments were acquired with 2048 complex data points in the t_2 dimension and 512 real free induction decays in the t_1 dimension using the States−TPPI mode as described previously (*15*). Spin-lock times of 40 ms (TOCSY) and a mixing time of 80 ms (NOESY) at a temperature of 30 °C were selected. Proton chemical shifts were referenced relative to internal DSS. ^{31}P NMR spectra were referenced to 85% phosphoric acid contained in a small glass sphere immersed in the sample.

All spectra were processed on a Silicon Graphics Indigo2 workstation using the software packages UXNMR (Bruker, Karlsruhe) for data processing and AURELIA (*16*) for data evaluation. Phosphorus spectra used for the equilibrium constant determination were filtered by an exponential window function causing no significant line broadening. Two-dimensional ^1H spectra were filtered by a sine bell window multiplication after zero filling in the indirect dimension and Fourier transformed to 1024 × 2048 (F_1 × F_2) real data points.

RESULTS

Monoglucosylation of Ras·GDP Observed by ^{31}P NMR. The influence of monoglucosylation of Ras by *C. sordellii* lethal toxin on the conformational states of the active center of Ras·GDP was first studied by ^{31}P NMR techniques in solution. Phosphorus NMR spectroscopy allows not only the direct observation of changes in the environment of the two phosphate groups of bound GDP but also the analysis of the reaction kinetics since LT converts UDP-glucose to free UDP and glucosylated protein. Thr35, the residue being glucosylated by LT, is located in the effector loop of the GTPase. It senses the GDP−GTP exchange and interacts directly with the magnesium ion and the terminal phosphate of GTP in the triphosphate-bound state of the molecule.

To follow the reaction kinetics, the glucosylation reaction was performed in the NMR sample tube using adequate protein amounts to record a single spectra within approximately 83 min. The time course of the glucosylation reaction on Ras·GDP by LT is shown in Figure 1. Before addition of the substrates of the enzymatic reaction (0′) only

Table 1: ^{31}P NMR Chemical Shifts of Ras·GDP·Mg^{2+} and Ras·GppNHp·Mg^{2+} upon Glucosylation of Thr35[a]

protein complex	chemical shifts δ (ppm)[b] α	β
UDP-glucose	−11.21	−12.79
UDP	−10.14	−6.06
Ras(wt)·GDP·Mg^{2+}	−10.68	−2.03
Ras(T35glc)·GDP·Mg^{2+}	−11.18	−2.26

protein complex	chemical shifts δ (ppm)[b] α(1)	α(2)	β(1)	β(2)	γ(1)	γ(2)
Ras(wt)·GppNHp·Mg^{2+}	−11.15	−11.85	−2.69	−3.41	−0.41	−0.23
Ras(T35glc)·GppNHp·Mg^{2+}[c]	−11.40		−2.55		−0.42	

[a] Experimental conditions as in Figures 1 and 3. Spectra were recorded at pH 7.4 and 20 °C for Ras·GDP and 15 °C for Ras·GppNHp, respectively. Chemical shift values for Ras(wt) are taken from ref *13*. [b] The resonances of states 1 and 2 are designated as α(1) and α(2), respectively. State 1 is defined as the state where the resonance of the β-phosphate group is shifted downfield relative to the second position. [c] Monoglucosylation of Thr35 selectively stabilizes the downfield-shifted state 1.

the signals of the α- and β-phosphate of Ras·GDP were detected but no signals of free GDP. Subsequently, UDP-glucose and LT toxin were added (Figure 1) to the solution. This led to the appearance of two new sets of ^{31}P NMR signals correponding to UDP-glucose and UDP. During the recording of the following 11 spectra (1 h 23 min to 15 h 14 min) the resonance signals for UDP increased due to the LT-catalyzed reaction [UDP-glucose + Ras·GDP → UDP + Ras(T35glc)·GDP]. The increase of UDP (α, −10.14 ppm; β, −6.06 ppm) was therefore used as a measure for the amount of glucosylated Ras protein. However, an increase of inorganic phosphate (P_i) and nucleotide monophosphate (UMP) could be observed during the time course of the measurements. After the total reaction time of 36 h the signals of UMP and UDP are vanished or diminished, respectively, indicating the hydrolysis of these compounds. The hydrolysis may be due to the instability of UDP-glucose and UDP or to small impurities of phosphatases originating from the nucleotide exchange procedure. Additionally, a small quantity of the inorganic phosphate may result from GDP released from degraded Ras protein. The ^{31}P chemical shift values are listed in Table 1.

As seen in Figure 1, we can observe chemical shift changes for the Ras-bound GDP upon monoglucosylation of Thr35. The resonance signal for the β-phosphate is shifted to higher field by about −0.23 ppm. This slight shift from "left to right" can be seen best for the spectrum recorded at 5 h 32 min where both forms of Ras, nonglucosylated Ras and glucosylated Ras, occur in almost equal concentrations. The observation of changes of the α-phosphate resonance is partly hidden by the signals of the UDP. However, from the spectra, which were recorded after the reaction was almost completed, it seems that the α-phosphate signal is shifted about −0.5 ppm to high field upon glucosylation. After 36 h reaction time approximately 80% of Ras is modified, as estimated from the integrals of the α-phosphate resonances in the modified and nonmodified protein.

Kinetics of the Monoglucosylation Reaction. The kinetics of the enzymatic reaction of LT for monoglucosylation of Ras was analyzed by integration of the well-resolved

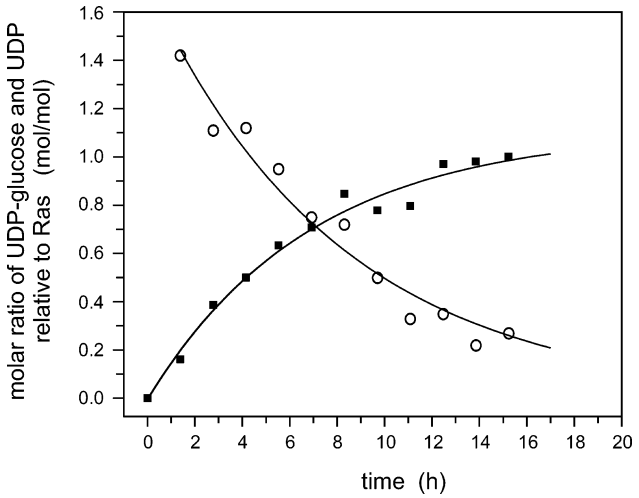

FIGURE 2: Kinetics of the Ras glucosylation reaction by LT. The production of UDP (filled squares) during the enzymatic glucosylation of Ras·GDP and the decrease of the cosubstrate UDP-glucose (open circles) were taken from the signal intensities of the β-phosphate groups, respectively, as shown in Figure 1. The molar ratios were determined relative to the signal intensity of the β-phosphate group from Ras·GDP and fitted to an exponential saturation equation assuming pseudo-first-order kinetics.

resonance signal of the β-phosphate group of UDP (β_{UDP}) at −6.06 ppm whose intensity increases with time. It is accompanied by a decrease of the intensity of the signal of the β-phosphate group of UDP-glucose ($\beta_{UDP-glucose}$) at −12.79 ppm. Unfortunately, the modification-induced chemical shift changes of the α- and β-phosphate resonance of the Ras-bound nucleotide are partly hidden or too small for a quantitative evaluation. For each spectrum the integrals of the signals of β_{UDP} and $\beta_{UDP-glucose}$ were normalized to the signal intensity of β-phosphate group of bound GDP ($\beta_{Ras-GDP}$). The ratio y of β_{UDP} or $\beta_{UDP-glucose}$ to $\beta_{Ras-GDP}$ was simulated as a function of the time t assuming pseudo-first-order kinetics (Figure 2). For the increase of UDP a least-squares fit [$y = A_0(1 - \exp(-kt))$] results in a time constant k of 0.145 ± 0.02 h^{-1}, which corresponds to a mean half-time of 4 h 47 min and a molar ratio A_0 of incorporated glucose of 1.08 ± 0.07. Simultaneously, the turnover of UDP-glucose to UDP and incorporated glucose corresponds to a time constant k of 0.123 ± 0.01 h^{-1} and a molar ratio A_0 of 1.71. Ideally, the decrease of the UDP-glucose signal should match exactly the increase in free UDP. Degradation of UDP to UMP or uridine and P_i would explain qualitatively the discrepancy observed. Indeed, UMP and inorganic phosphate are produced during the observation time, probably by the presence of traces of phosphatases in the sample. However, since only approximately 80% of Ras are modified (see above), additional UDP-glucose has to be hydrolyzed during the reaction time. This could occur by a side reaction of LT where either glucose from UDP-glucose is transferred directly to water instead to the threonine hydroxyl group or glucose is removed from glucosylated threonine by LT in a partial reversal of the reaction.

The obtained pseudo-first-order time constant appears with 0.145 h^{-1}, rather small for physiological conditions. However, because of experimental requirements the reaction was performed at very low toxin concentrations (11.4 nM) compared to the Ras concentration (0.47 mM) at a temperature of 20 °C, well below a temperature which is physi-

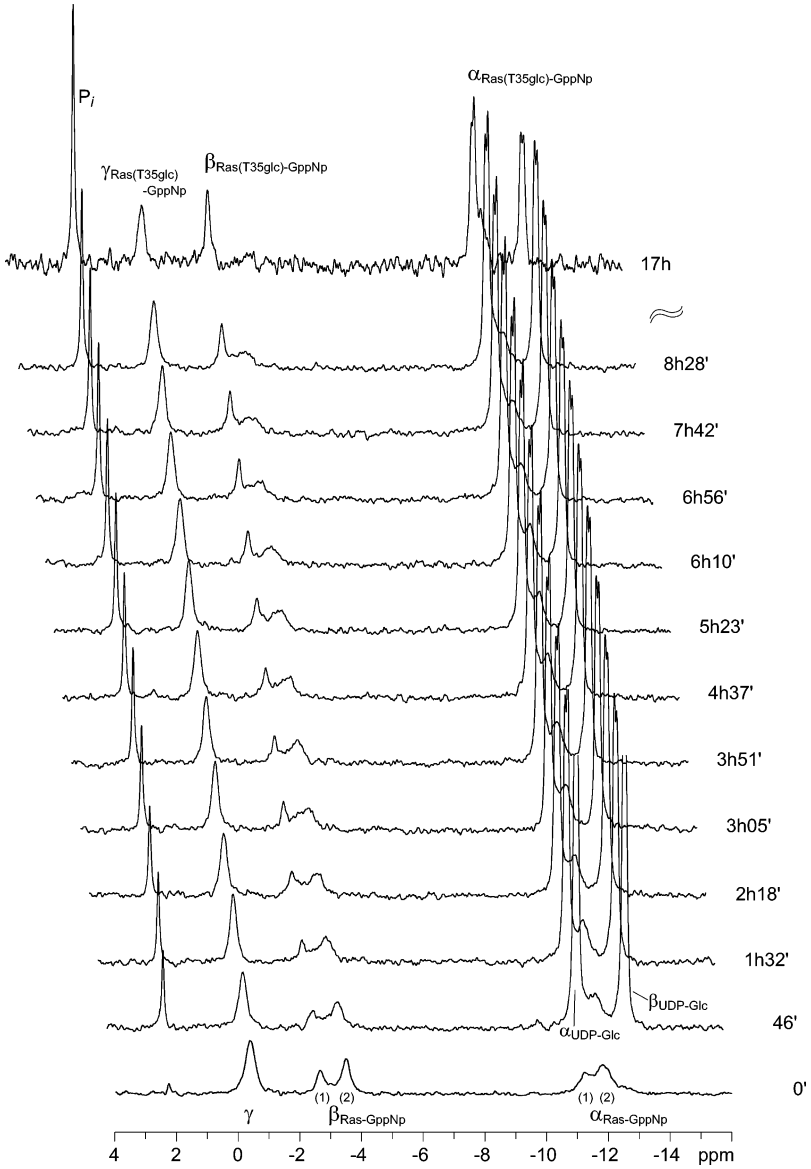

FIGURE 3: Monoglucosylation of Ras·GppNHp·Mg^{2+} by LT. Spectra were recorded at 15 °C in 20 mM Tris-HCl buffer at pH 7.4 using a total protein concentration of 0.95 mM Ras·GppNHp·Mg^{2+} and 13 nM LT toxin with 2.4 mM UDP-glucose, 5 mM $MgCl_2$, 120 mM NaCl, and 140 mM KCl in 750 μL of water (H_2O/D_2O, 90%/10%). For each single spectra 640 scans were recorded, taking 46 min each. Note the splitting of the α- and β-phosphate groups due to a conformational change in the effector loop of Ras and the subsequent stabilization of state 1 upon Thr35 glucosylation. ^{31}P resonance signals of free UDP are not observed because of phosphatase activity due to the GppNHp nucleotide exchange procedure.

ological for mammals. Assuming that at small times optimum (v_{max}) conditions exist, a turnover number k_{cat} of >1.8 s^{-1} can be estimated from the data.

Conformational Transitions of Ras·GppNHp Induced by Monoglucosylation at Threonine-35. Next, we analyzed the ability of LT to glucosylate Ras in its nucleoside triphosphate form. In these experiments GTP was replaced by the stable GTP analogue GppNHp. It has been shown previously that Ras exists in two conformational states when bound to GppNHp. These states were assigned to an open (state 1) and closed (state 2) conformation (*13*). We first recorded a spectrum of Ras·GppNHp showing two sets of resonance lines for the β- and α-phosphate groups (Figure 3, time point 0′) corresponding to the two conformational states. Then a 2.5-fold excess of UDP-glucose to Ras and catalytic amounts of LT were added at 15 °C. During the following 8 h the resonance signal of the β-phosphate group assigned to the open conformation (state 1) increased, while the signal corresponding to state 2 decreased with the time.

Although the α-phosphate resonance was partly hidden by the signals of UDP-glucose, the decrease of the high-field-shifted line corresponding to state 2 was clearly visible. After several hours Ras was fully glucosylated, and only one set of resonance lines could be observed for Ras(T35glc)·GppNHp. Here, a rate constant for the monoglucosylation is 0.076 ± 0.01 h^{-1}, which corresponds to a mean half-time of 9 h 5 min. This 2-fold decrease in the time constant compared to the GDP experiment may mainly be the result of the different Ras to LT ratio and a lower reaction temperature. Since the two states can only be observed by NMR at lower temperatures, the temperature was reduced to 15 °C. The turnover rate of the modification k_{cat} estimated under the assumption that almost optimal conditions exist at small times is >1.4 s^{-1}, comparable to that of Ras·GDP.

From the chemical shift values observed for the glucosylated protein its conformation would correspond to state 1 (Figure 3, top spectrum). The NMR signals of the reaction product UDP could not be observed, most likely because of traces of phosphatases that remain from the nucleotide exchange procedure. The glucosylation reaction of the Ras protein was confirmed by mass spectrometry (data not shown). As mentioned above, X-ray crystallography reveals that the hydroxyl group of Thr35 is involved in a hydrogen bond to the γ-phosphate group of GppNHp and thus should not be accessible for glucosylation. However, the reaction observed requires an intrinsic flexibility of the effector loop that provides the accessibility of the Thr35 side chain for the substrate.

Identification of the Signals of Ras-T35 Glucose Reveals the α*-Anomeric Configuration for the Bound Hexose.* The enzymatic reaction of the Ras monoglucosylation by LT requires the cleavage of the UDP-glucose cosubstrate and a covalent attachment of the hexose to the hydroxyl group of the side chain of Thr35. In UDP-glucose the glucose moiety is linked to the phosphate group of UDP in its α-anomeric form. To further understand this mechanism, it is of high interest to analyze the configuration of the glycosidic bond to Ras since an isomerization reaction could occur during the transfer to Thr35. NMR spectroscopy is a suitable technique to determine the isoform of a glycosidic bond from the chemical shifts and the *J*-coupling value of the C1′ hydrogen. For α-anomeric configurations of hexoses in aqueous solutions the C1−H resonance is typically found at 5.3 ppm, showing a ^3J-coupling value to C2−H between 2 and 5 Hz (glucose 3.7 Hz), while for β-anomeric configurations the C1−H resonance is found at 4.7 ppm with a *J*-coupling value between 7 and 9 Hz (glucose 7.9 Hz) (*17*). Usually, in aqueous solution 60% of glucose occurs in the β-anomeric configuration and 40% in the α-anomeric configuration at C1.

We first recorded one-dimensional ^{1}H NMR spectra of Ras·GDP in the glucosylated and nonglucosylated forms (Figure 4). Since the enzymatic reaction by LT requires high salt buffer conditions, which are not favorable for NMR spectroscopy, and since the concentrations of free nucleotides should be reduced, we dialyzed the sample after reaction with LT three times against phosphate buffer containing low amounts to no DTE. We then lyophilized the protein and redissolved it in D_2O. Under these conditions some high-field-shifted H^α resonances of Ras and the C1′−H of Ras-bound GDP can be observed. Not only are direct sequential neighbors of Thr35 affected by the glucosylation reaction, but also residues further away in the sequence show chemical shift changes (Figure 4). These include residues in the joining β-strand β2, namely, Ser39 and Gln43. The resonance assignment is based on published data (*18*, *19*). To confirm the line shifts, we performed a glucosylation by LT with slightly less than equimolar concentrations of UDP-glucose to Ras and dialyzed the sample against phosphate buffer. This resulted in approximately 80% Ras(T35glc)·GDP and 20% unmodified Ras·GDP. As can be seen in the middle spectrum of Figure 4, unmodified and monoglucosylated Ras protein can be distinguished by the separate resonance lines of Ser39 and the shift of Gln43.

To identify the chemical shifts of the covalently bound glucose, we next performed 2D correlation experiments using

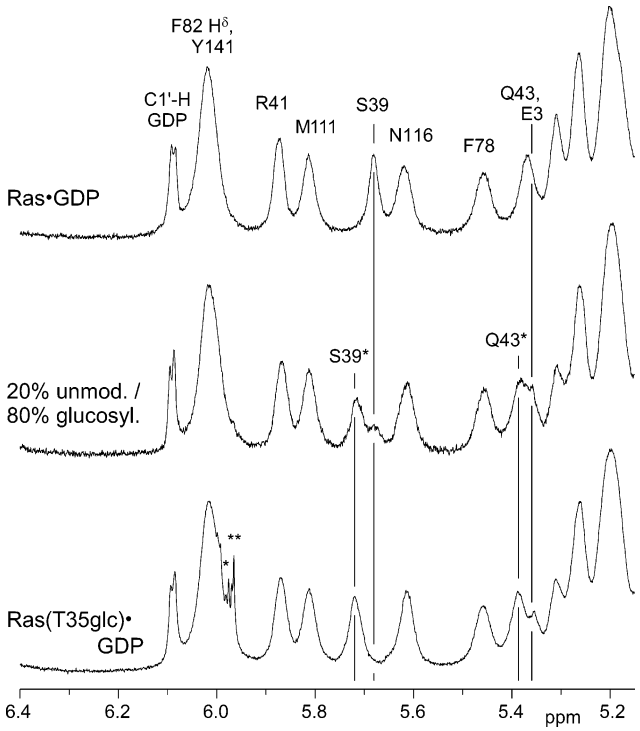

FIGURE 4: Part of the H^α chemical shift region of ^{1}H NMR spectra of unmodified and monoglucosylated Ras at 800 MHz. Spectra were recorded in 50 mM Tris-HCl buffer and 5 mM $MgCl_2$, pH 7.0, in D_2O at 30 °C. Chemical shift changes of S39 and Q43 indicate conformational changes upon glucosylation in β-strand β2. Resonance signals labeled with * and ** in the bottom spectrum correspond to the ribose C1′−hydrogen shift of the UDP-glucose substrate and UDP, respectively.

the 80% glucosylated Ras·GDP sample described above. We used this sample in order to avoid potential signal overlap with the small substrates UDP-glucose or free glucose which was not completely removed by dialysis. As seen in the overlay spectra there is only one new set of resonances with a coupling pattern typical for a glucose moiety. This allows identification of the spin system for the bound glucose moiety from homonuclear TOCSY experiments (Figure 5). Importantly, the chemical shift of the C1′ hydrogen at 5.00 ppm would be in line with the α-anomeric form of the bound glucose. As a control we recorded 2D correlation spectra of free UDP-glucose in the same buffer that show the resonance line of the C1′ hydrogen at 5.61 ppm and the resonances of the other glucose hydrogens in the range of 3.93−3.45 ppm (data not shown). These shifts are clearly distinct from the glucose spin system identified in the protein spectra.

Unfortunately, we could not determine the *J*-coupling value for C1′−H because of signal overlap in the 1D spectrum and limited frequency dispersion in the 2D spectra. However, the *J*-coupling was supposed to be small since we could resolve doublet lines in the 2D spectra down to 5 Hz, supporting the α-anomeric form of the glucose. Additionally, we observed a shift of the Ser39 resonances upon glucosylation and other resonance lines as already described in the 1D spectra shown in Figure 4.

Urea Denaturation Experiments Confirm the α*-Anomeric Linkage of the Thr35Glc Moiety.* As additional proof for the configuration of the bound glucose we denatured the sample containing 80% glucosylated Ras with urea. To this end, we added deuterium-exchanged urea powder in three steps to a

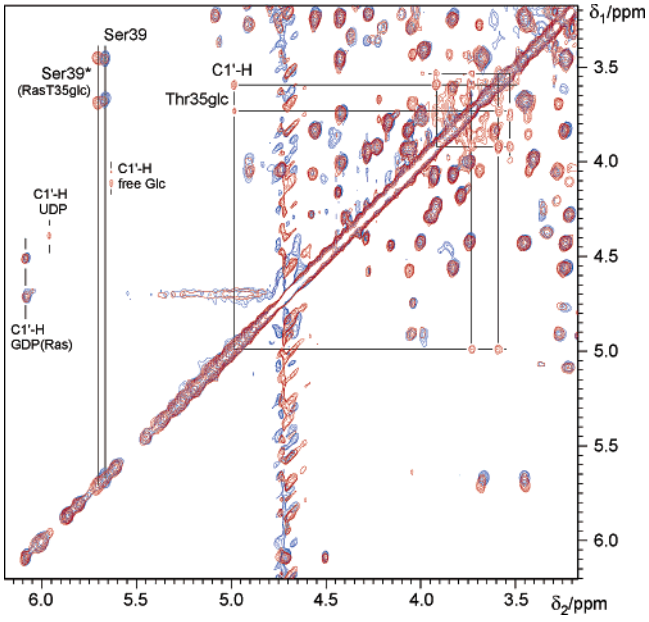

FIGURE 5: Overlay plot of ^{1}H TOCSY NMR spectra of monoglucosylated (red) and unmodified Ras·GDP·Mg^{2+} (blue). Spectra were recorded in 50 mM Tris-HCl buffer, pH 7.0, in D_2O with 5 mM $MgCl_2$ at 30 °C. No DTE was added in order to prevent overlay with glucose proton resonance signals. The protein concentration was varied between 1.4 mM for the glucosylated sample and 2.0 mM for the nonglucosylated sample. The spin system of the glucose linked to the Thr35 hydroxyl group is marked. Additional signals of C1′ hydrogens for Ras-bound GDP, free UDP, and glucose are labeled.

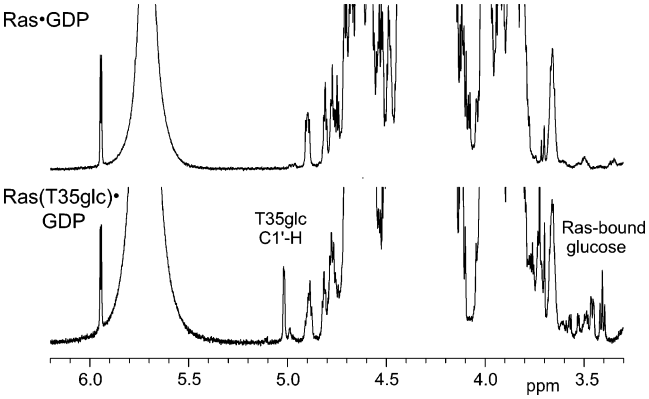

FIGURE 6: ^{1}H NMR spectra of urea-denatured nonmodified Ras·GDP and monoglucosylated Ras(T35glc)·GDP. Spectra were recorded after addition of 8 M urea in D_2O at 50 °C. Resonance lines of the sugar moiety can be identified and reveal the α-anomeric conformation of the covalently attached glucose by chemical shift position and *J*-coupling value.

final concentration of 8 M and heated the sample to 50 °C. It turned out that the Ras protein is surprisingly stable and resistant to urea denaturation; however, after 60 min at elevated temperature the protein was completely unfolded. The high stability of the Ras is reminiscent of a previous observation when the protein was titrated from physiological pH to pH 2.2 and shown to keep its native structure (*20*). Here, as a control for the identification of the glucose signal we performed the same procedure with nonglucosylated Ras. The H^{α} part of the spectra obtained for the two samples is shown in Figure 6. A comparison reveals that both spectra are essentially identical besides the appearance of the resonance lines of the bound glucose at 5.02 ppm and around

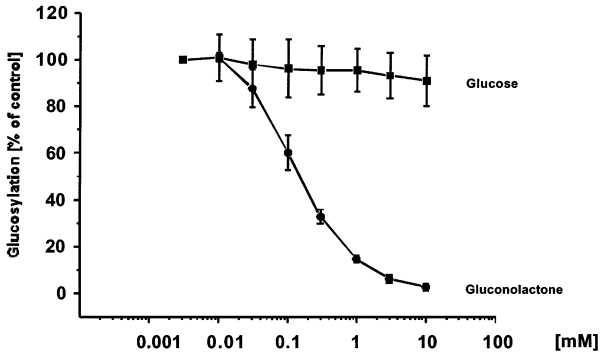

FIGURE 7: Gluconolactone inhibits the glucosylation of H-Ras by lethal toxin. H-Ras was glucosylated by lethal toxin (10 nM) in the presence of 10 μM UDP-[^{14}C]glucose with increasing concentrations of 1,5-gluconolactone (filled circles) or glucose (filled squares). Labeled protein was separated by SDS−PAGE and radioactivity incorporated determined by phosphorimaging. Given is the amount of label as compared to maximal ^{14}C-glucosylation. 1,5-Gluconolactone but hardly any glucose blocked the incorporation of radioactivity into H-Ras. The experiment was performed three times with similar results.

3.5 ppm. The *J*-coupling of the C1′ hydrogen was determined to 3.2 Hz, which is in agreement with an α-anomeric configuration at C1′. No sign of a second C1′ resonance corresponding to the *β*-anomer could be observed.

The analysis of the ^{1}H NMR experiments leads to the conclusion that monoglucosylation of Ras by LT changes the conformation of the effector loop and the joined *β*2 strand and that the glucose is attached to the side chain of Thr35 in the α-anomeric configuration without observable isomerization.

Inhibition of Glucosylation by Gluconolactone. To obtain further insights into the catalytic mechanism of the glucosylation of Ras induced by LT, we studied the effects of 1,5-gluconolactone on the LT activity. When gluconolactone was added at increasing concentrations to the glucosylation mixture, the modification of Ras was inhibited in a concentration-dependent manner (Figure 7). By contrast, glucose added at a similar concentration as gluconolactone did not inhibit the LT-catalyzed glucosylation of Ras.

DISCUSSION

Large clostridial cytotoxins modify small GTPases of the Rho and Ras family by glucosylation (*C. difficile* toxins A, B, and LT) and by *N*-acetylglucosaminylation (*C. novyi* α-toxin). Whereas most toxins of this family specifically modify Rho proteins, *C. sordellii* lethal toxin and isoforms of toxin B (e.g., subtype 1470) glucosylate also Ras subfamily proteins including Ras, Rap, and Ral. Glucosylation of Rho GTPases by large clostridial toxins occurs at Thr35/37. The same residue (Thr35) is modified in Ras by LT. Here the functional consequences of the glucosylation of H-Ras by LT were studied by ^{31}P and ^{1}H NMR.

Monoglucosylation of Ras Stabilizes the Effector Nonbinding State. Essential for the signaling function of Ras are major conformational changes in the switch regions that occur upon binding of nucleoside di- or triphosphates (*14*). We have shown previously that Ras·GppNHp exists in two conformational states within the effector loop that are in mutual exchange in the millisecond time scale (*13*). The two conformations observed were assigned to an open conforma-

tion (state 1) with Tyr32 being further apart from the phosphate groups as found in the high-resolution crystal structure of free Ras·GppNHp (*9*) and a closed conformation (state 2) with Tyr32 forming a hydrogen bound with its side chain hydroxyl to the γ-phosphate group as found in the Rap1A−Raf complex structure (*21*). The dynamics of the switch regions is preserved even in the crystallized protein (*22*), while association of the effector protein Raf or the GTPase activating protein RasGAP to Ras mutually stabilize the closed or open state, respectively (*13*). Thr35, which is highly conserved among the superfamily of small GTPases, has a key function for the flexibility and conformation of the effector loop since its side-chain hydroxyl group is coordinated to the magnesium ion and its amide group to the γ-phosphate in the nucleoside triphosphate bound form of the GTPase (*9*). Mutation of this critical threonine to serine or alanine previously used as partial loss-of-function mutations in cell-based assays shows a reduced affinity to Ras effectors although Thr35 is not being involved in any direct protein−protein interaction. However, as could be shown by NMR spectroscopy, they drastically affect the dynamic behavior of the effector loop and therewith the binding to effectors (*13*, *23*).

Most probably in state 1 of wild-type Ras·GppNHp the coordination of Thr35 to the nucleotide−Mg^{2+} complex in the active center is abolished. We therefore investigated by NMR spectroscopy the effect of monoglucosylation of Ras at Thr35 with GDP or GppNHp bound on the conformation of the protein.

In Ras·GDP glucosylation of Thr35 led to upfield shifts of the α- and β-phosphate resonances by 0.5 and 0.23 ppm, respectively. These spectral changes indicate a change of the environment of the phosphate group by the modification which probably reflects the close proximity of the modification to the phosphate groups of GDP. However, this perturbation is rather small and would be in agreement with the high conformational flexibility of the switch regions reported earlier (*24*). The shift changes are reminiscent of the observation of two conformational states that have been previously detected also for Ras·GDP (*25*) as well as for other GTPases, e.g., Ran (*26*). The glucosylation may perturb the flexibility and thus shift the average structure of the switch regions, mainly affecting the effector loop. Interestingly, we could observe chemical shift changes (indicative for conformational changes) even in the residues Ser39 and Gln43 further apart from Thr35 by ^{1}H NMR. For the GDP complex of Ras glucosylated by LT an X-ray structure has been published (*12*). According to this structure, these residues are located at the solvent-exposed site of the second β-strand of Ras that forms the intermolecular β-sheet with effectors (Figure 8). Importantly, Ser39 contributes to the stabilization of the Ras−Raf complex by formation of four hydrogen bonds to Arg89 and Arg67 of Raf (*21*). The small changes induced by glucosylation in the accompanying β-strand may therefore explain why this modification inhibits Ras signaling, although Thr35 is not involved in any direct interaction with the kinase.

Nevertheless, glucosylation of Ras·GDP leads to an additional decrease of the affinity to Raf-RBD by almost 2 orders of magnitude (from 45 to <1 mM^{-1}) (*11*), which is most probably not a direct steric hindrance of the effector interaction by the glucosyl moiety. Interestingly, Ser39 in

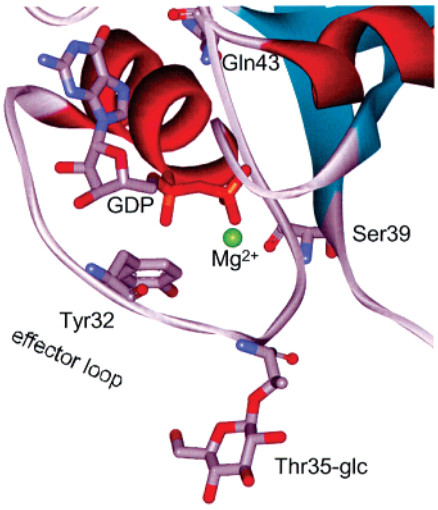

FIGURE 8: Structure of the glucosylated Ras(T35glc)·GDP protein with the glucose in the α-anomeric conformation. The structural model is based on the coordinates of the X-ray structure of glucosylated Ras·Mg^{2+}·GDP (12). The flexible loops L1, L2 (effector loop), and L4 surrounding the two phosphate groups of GDP are labeled as well as residues Tyr32, Thr35, and Ser39. The figure was generated with WebLab Viewer (Accelrys Inc.).

Ras corresponds to Asn41 in RhoA, which is ADP-ribosylated by the C3 exoenzyme. Glucosylation of Thr37 by toxin B is known to inhibit the ribosylation at position 41 (*6*, *27*). These observations suggest structural changes in the effector loop upon glucosylation that extend to strand β2. Thus, the chemical shift changes observed for Ser39 upon Ras monoglucosylation remind us of large conformational changes observed in the crystal structure of RhoA·GTPγS compared to Ras−nucleoside triphosphate structures that are thought to explain the block of Asn41 ribosylation after Thr37 glucosylation (*28*).

In the nucleoside triphosphate form ^{31}P NMR spectroscopy indicates a stabilization of state 1, which has been previously assigned to the open conformation of the effector loop. Again, these data nicely correlate with the observation that glucosylated Ras does not interact with Raf effectors, since all Ras effector domains studied so far are known to bind Ras only in its closed confirmation (state 2), where both Thr35 and Tyr32 are coordinated to the nucleoside triphosphate−magnesium complex (*13*, *15*, *21*, *23*, *29*, *30*). It has been postulated earlier that in state 1 the hydroxyl group of Thr35 is not coordinated to the metal ion (*23*). This would imply that this group is accessible to LT and can be modified when GppNHp is bound, as is indeed observed here. Conversely, the ^{31}P chemical shift changes after modification of Thr35 are very similar to those induced by mutation of Thr35 and thus confirm our structural model for state 1 (*23*). It will be of interest to analyze the glucosylation reaction for other nucleoside triphosphate analogues, e.g., GTPγNH_2, that are known to preserve the dynamic behavior of Ras (*31*).

We could obtain an estimate of the turnover number for the modification of Ras·GDP from the NMR data as ≥ 1.8 s^{-1} at 20 °C, a value which is in line with published values obtained by biochemical methods. Busch et al. (*32*) found a k_{cat} of 0.33 and 4.9 s^{-1} for Rac·GDP and Ras·GDP, respectively, at 37 °C. For the Ras·GppNHp complex we found a k_{cat} of ≥ 1.4 s^{-1} at 15 °C, which is close to the value found for Ras·GDP. This would fit well to our picture that

the hydroxyl group of Thr35 is accessible by LT in state 1. State 1 is in fast equilibrium with state 2 within a time scale of milliseconds; it is not a rate-limiting step under our conditions.

Catalytic Mechanism of LT. Analysis of the proton chemical shifts of the incorporated glucose suggests the α-anomeric configuration for the attached glucose. This observation is in agreement with a published crystal structure of Ras(T35glc)·GDP where only α-anomeric glucose could be fitted into the electron density map (*12*). NMR spectroscopy reveals that the reaction is highly stereospecific since no racemization was observable in solution. This is important since crystallization could select for one anomer of glucose although both anomers are present in the solution. The α-anomeric linkage of the glucose moiety to the hydroxyl group of Thr35 suggests that the transfer reaction must occur under retention of the configuration of the α-D-glucose at the C1′ position. The retention of the glucose configuration excludes an enzymatic mechanism that results in an inversion of the chiral center, e.g., a single S_N2 reaction mechanism. As discussed by Vetter et al. (*12*) a binucleophilic substitution (double displacement) or, alternatively, a stereospecific S_N1 reaction could be performed by the LT enzyme, where the catalytic pocket of the toxin prevents formation of a racemate. However, as we show LT can be inhibited by 1,5-gluconolactone. This indicates that the reaction mechanism of LT may include a glucosyl oxocarbonium ion transition state as is suggested for the glycogen synthase that also uses UDP-glucose during the glycogen synthesis (*33*). Here, the transition state analogue 1,5-gluconolactone is an inhibitor of the glycogen synthesis. A similar mechanism is also proposed for the glycogen phosphorylase and lysozyme which are both inhibited by 1,5-gluconolactone.

ACKNOWLEDGMENT

We thank Ingrid Vetter for providing the coordinates of glucosylated Ras·GDP.

REFERENCES

1. Arseculeratne, S. N., Panabokke, R. G., and Wijesundera, S. (1969) *J. Med. Microbiol. 2*, 37−53.
2. Busch, C., and Aktories, K. (2000) *Curr. Opin. Struct. Biol. 10*, 528−535.
3. Green, G. A., Schué, V., and Monteil, H. (1995) *Gene 161*, 57−61.
4. Kelly, C. P., and LaMont, J. T. (1998) *Annu. Rev. Med. 49*, 375−390.
5. Kelly, C. P., Pothoulakis, C., and LaMont, J. T. (1994) *New Engl. J. Med. 330*, 257−262.
6. Just, I., Selzer, J., Wilm, M., von Eichel-Streiber, C., Mann, M., and Aktories, K. (1995) *Nature 375*, 500−503.
7. Just, I., Selzer, J., Hofmann, F., Green, G. A., and Aktories, K. (1996) *J. Biol. Chem. 271*, 10149−10153.
8. Selzer, J., Hofmann, F., Rex, G., Wilm, M., Mann, M., Just, I., and Aktories, K. (1996) *J. Biol. Chem. 271*, 25173−25177.
9. Pai, E. F., Krengel, U., Petsko, G. A., Goody, R. S., Kabsch, W., and Wittinghofer, A. (1990) *EMBO J. 9*, 2351−2359.
10. Popoff, M. R., Chaves-Olarte, E., Lemichez, E., von Eichel-Streiber, C., Thelestam, M., Chardin, P., Cussac, D., Antonny, B., Chavrier, P., Flatau, G., Giry, M., de Gunzburg, J., and Boquet, P. (1996) *J. Biol. Chem. 271*, 10217−10224.
11. Herrmann, C., Ahmadian, M. R., Hofmann, F., and Just, I. (1998) *J. Biol. Chem. 273*, 16134−16139.
12. Vetter, I. R., Hofmann, F., Wohlgemuth, S., Herrmann, C., and Just, I. (2000) *J. Mol. Biol. 301*, 1091−1095.
13. Geyer, M., Schweins, T., Herrmann, C., Prisner, T., Wittinghofer, A., and Kalbitzer, H. R. (1996) *Biochemistry 35*, 10308−10320.
14. Vetter, I. R., and Wittinghofer, A. (2001) *Science 294*, 1299−1304.
15. Geyer, M., Herrmann, C., Wohlgemuth, S., Wittinghofer, A., and Kalbitzer, H. R. (1997) *Nat. Struct. Biol. 4*, 694−699.
16. Neidig, K. P., Geyer, M., Görler, A., Antz, C., Saffrich, R., Beneicke, W., and Kalbitzer, H. R. (1995) *J. Biomol. NMR 6*, 255−270.
17. Fribolin, H. (1999) *Basic one- and two-dimensional NMR spectroscopy*, Wiley-VCH, New York.
18. Muto, Y., Yamasaki, K., Ito, Y., Yajima, S., Masaki, H., Uozumi, T., Wälchli, M., Nishimura, S., Miyazawa, T., and Yokoyama, S. (1993) *J. Biomol. NMR 3*, 165−184.
19. Ito, Y., Yamasaki, K., Iwahara, J., Terada, T., Kamiya, A., Shirouzu, M., Muto, Y., Kawai, G., Yokoyama, S., Laue, E. D., Walchli, M., Shibata, T., Nishimura, S., and Miyazawa, T. (1997) *Biochemistry 36*, 9109−9119.
20. Schweins, T., Geyer, M., Scheffzek, K., Warshel, A., Kalbitzer, H. R., and Wittinghofer, A. (1995) *Nat. Struct. Biol. 2*, 36−44.
21. Nassar, N., Horn, G., Herrmann, C., Scherer, A., McCormick, F., and Wittinghofer, A. (1995) *Nature 375*, 554−560.
22. Stumber, M., Geyer, M., Graf, R., Kalbitzer, H. R., Scheffzek, K., and Haeberlen, U. (2002) *J. Mol. Biol. 323*, 899−907.
23. Spoerner, M., Herrmann, C., Vetter, I. R., Kalbitzer, H. R., and Wittinghofer, A. (2001) *Proc. Natl. Acad. Sci. U.S.A. 98*, 4944−4949.
24. Kraulis, P. J., Domaille, P. J., Campbell-Burk, S. L., van Aken, T., and Laue, E. D. (1994) *Biochemistry 33*, 3515−3531.
25. Rohrer, M., Prisner, T. F., Brügmann, O., Käss, H., Spoerner, M., Wittinghofer, A., and Kalbitzer, H. R. (2001) *Biochemistry 40*, 1884−1889.
26. Geyer, M., Assheuer, R., Klebe, C., Kuhlmann, J., Becker, J., Wittinghofer, A., and Kalbitzer, H. R. (1999) *Biochemistry 38*, 11250−11260.
27. Just, I., Richter, H. P., Prepens, U., von Eichel-Streiber, C., and Aktories, K. (1994) *J. Cell Sci. 107*, 1653−1659.
28. Ihara, K., Muraguchi, S., Kato, M., Shimizu, T., Shirakawa, M., Kuroda, S., Kaibuchi, K., and Hakoshima, T. (1998) *J. Biol. Chem. 273*, 9656−9666.
29. Linnemann, T., Geyer, M., Jaitner, B. K., Block, C., Kalbitzer, H. R., Wittinghofer, A., and Herrmann, C. (1999) *J. Biol. Chem. 274*, 13556−13562.
30. Herrmann, C. (2003) *Curr. Opin. Struct. Biol. 13*, 122−129.
31. Stumber, M., Herrmann, C., Wohlgemuth, S., Kalbitzer, H. R., Jahn, W., and Geyer, M. (2002) *Eur. J. Biochem. 269*, 3270−3278.
32. Busch, C., Hofmann, F., Gerhard, R., and Aktoris, K. (2000) *J. Biol. Chem. 275*, 13228−13234.
33. Kim, S. C., Singh, A. N., and Raushel, F. M. (1988) *J. Biol. Chem. 263*, 10151−10154.

BI034529V